X-ray Photoemission from the Creutz-Taube Mixed Valence Complex: A Reassessment

P. H. Citrin* and A. P. Ginsberg*

Contribution from Bell Laboratories, Murray Hill, New Jersey 07974.
Received November 6, 1980

Abstract: X-ray photoemission from the bromide and tosylate salts of the mixed valence complex cation $[(NH_3)_5Ru^{II}(pyr)Ru^{III}(NH_3)_5]^{+5}$ (denoted [II,III]) shows two Ru core level photopeaks with binding energies close to those in the [II,II] and [III,III] systems with relative integrated intensities of 1.0:1.0 ± 0.1. This is obviously consistent with a trapped valence dimer. However, the same spectrum is also predicted by a model for X-ray photoemission from a *delocalized* ground-state mixed valence dimer when account is taken of the high polarizability of the delocalized valence orbital and the expected large decrease in the electron coupling integral in the photoionized state. X-ray photoelectron spectroscopy therefore fails to distinguish between a localized and a delocalized ground state for this system. In general, a mixed valence dimer will give the same X-ray photoemission spectrum whether it has a localized ground state (Robin-Day class II) or is delocalized (class III) but has relatively weak metal-metal interaction.

Introduction

It is now over a decade since Creutz and Taube[1] reported the pyrazine-bridged binculear ruthenium complexes $[(NH_3)_5Ru(pyr)Ru(NH_3)_5]^{n+}$ (pyr = pyrazine, n = 4, 5, 6), in which the formal oxidation states of the ruthenium atoms may be written [II,II], [II,III], and [III,III]. The [II,III] mixed valence complex has attracted considerable attention involving a variety of theoretical and experimental studies.[2-15] In spite of this work the nature of the electronic ground state of the complex remains controversial. The discussion centers on whether the ground state is symmetric or asymmetric, that is, whether the unpaired 4d electron is best described as being trapped on one Ru site or delocalized over both sites. In terms of Robin and Day's classification of mixed valence compounds[16] the question is whether the [II,III] dimer belongs to class II (localized valence electrons with weak metal-metal interaction) or class III (delocalized valence electrons).

The major argument for a delocalized ground state in the [II,III] complex comes from analysis of its near-IR spectrum. A band at 6.4 kK, absent from the spectra of the [II,II] and [III,III] complexes, was originally assigned as an intervalence charge-transfer absorption[1] expected for a trapped valence complex.[1,3,6] Recently, however, Piepho, Krausz, and Schatz have developed a vibronic coupling model for calculating mixed valence absorption profiles, and application of this model to the 6.4-kK band provides strong evidence that the ground state of the [II,III] complex is delocalized.[12-14] The same conclusion was reached earlier by Hush[8] on the basis of a less rigorous analysis.[13] In conflict with this conclusion are a number of experiments which were interpreted as pointing to a localized ground state. None of these experiments or interpretations is free from criticism. For example, the reported Mössbauer spectra[5] are too poorly defined to be interpreted with confidence, and the powder EPR measurements,[11] which point to a localized ground state, have been contradicted by single-crystal measurements.[15]

What appeared to be definitive evidence for a trapped valence ground state was provided by an X-ray photoelectron spectroscopy (XPS) study of the [II,II], [II,III], and [III,III] dimer tosylate salts.[4] Two Ru core level photopeaks of equal integrated intensity with binding energies close to those in the pure [II,II] and [III,III] systems were observed for the mixed valence complex. This is clearly consistent with a localized ground state in which intersite electron exchange of the trapped valence is slow on the very short XPS measurement time scale ($\sim 10^{-17}$ s). However, Hush[7] subsequently pointed out that a delocalized mixed valence dimer can also give rise to two photopeaks with binding energies close to those of the separate ions. This is a consequence of the high polarizability expected for the delocalized valence orbital in such a complex. Under the influence of a core hole this orbital relaxes strongly and the system becomes localized. There are then two photoionized states, a lower one in which the valence electron is localized on the same center as the core hole, and an upper one in which it is on the other center. Hush proposed a simple model which gives the relative intensities of the photopeaks corresponding to these two states as a function of the electron coupling integral in the ground state.

As a consequence of Hush's analysis it is clear that a detailed interpretation is required in order to determine whether X-ray photoemission from a mixed valence complex can provide information about its ground state. It is the purpose of this paper to provide such an assessment for the Creutz-Taube mixed valence complex. To this end we have made a careful study of the Ru 3d and 3p X-ray photoelectron spectra of the [II,II], [II,III], and [III,III] dimers both as the bromide and tosylate salts. Particular attention was paid to the method of sample preparation and to the possible effects of radiation damage in order to demonstrate that the observation of two peaks in the spectrum is not an experimental artifact. Least-squares analyses of the Ru 3p spectra were performed to determine reliable relative intensities of the Ru(II) and Ru(III) components. Analysis of these intensities in terms of the Hush model[7] shows that they are consistent only with a localized ground state, as originally proposed.[4] However, if Hush's model is modified to allow for the expected large difference in electron coupling in the ground and photoionized states, it then becomes clear that the observed spectra are also consistent with a delocalized ground state. Our final conclusion is that the X-ray

(1) C. Creutz and H. Taube, *J. Am. Chem. Soc.*, **91** 3988 (1969); **95**, 1086 (1973).
(2) J. H. Elias and R. S. Drago, *Inorg. Chem.*, **11**, 415 (1972).
(3) B. Mayo and P. Day, *J. Am. Chem. Soc.*, **94**, 2885 (1972).
(4) P. H. Citrin, *J. Am. Chem. Soc.*, **95**, 6472 (1973).
(5) C. Creutz, M. L. Good, and S. Chandra, *Inorg. Nucl. Chem. Lett.*, **9**, 171 (1973).
(6) B. Mayo and P. Day, *Inorg. Chem.*, **13**, 2272 (1974).
(7) N. S. Hush, *Chem. Phys.*, **10**, 361 (1975).
(8) J. K. Beattie, N. S. Hush, and P. R. Taylor, *Inorg. Chem.*, **15**, 992 (1976).
(9) T. C. Strekas and T. G. Spiro, *Inorg. Chem.*, **15**, 974 (1976).
(10) J. K. Beattie, N. S. Hush, P. R. Taylor, C. L. Raston, and A. H. White, *J. Chem. Soc., Dalton Trans.*, 1121 (1977).
(11) B. C. Bunker, R. S. Drago, D. N. Hendrickson, R. M. Richman, and S. L. Kessel, *J. Am. Chem. Soc.*, **100**, 3805 (1978).
(12) S. B. Piepho, E. R. Krausz, and P. N. Schatz, *J. Am. Chem. Soc.*, **100**, 2996 (1978).
(13) K. Y. Wong, P. N. Schatz, and S. B. Piepho, *J. Am. Chem. Soc.*, **101**, 2793 (1979).
(14) K. Y. Wong and P. N. Schatz, *Prog. Inorg. Chem.*, **28**, in press.
(15) N. S. Hush, A. Edgar, and J. K. Beattie, *Chem. Phys. Lett.*, **69**, 128 (1980).
(16) M. B. Robin and P. Day, *Adv. Inorg. Chem. Radiochem.*, **10**, 247 (1967).
(17) (a) M. S. Lazarus and T. K. Sham, *J. Am. Chem. Soc.*, **101**, 7622 (1979). (b) C. Battistoni, C. Furlani, G. Mattogno, and G. Tom, *Inorg. Chim. Acta*, **21**, L25 (1977).

0002-7863/81/1503-3673$01.25/0

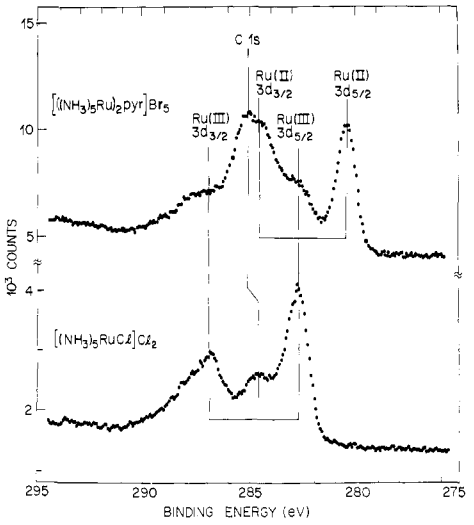

Figure 1. Ru 3d XPS spectra in monovalent $[(NH_3)_5RuCl]Cl_2$ (bottom) and the mixed valence Creutz–Taube complex (top). Note the presence of more than one component in the latter and the difficulty in determining individual relative peak intensities. Samples mounted by gentle pressing onto Au substrates.

photoelectron spectrum of the [II,III] complex does not provide useful information about its ground state. This conclusion may be generalized to the statement that XPS studies of mixed valence dimers cannot distinguish between class II compounds and class III compounds in which the metal–metal interaction is relatively weak.

Experimental Section

The tosylate and bromide salts of the [II,II], [II,III], and [III,III] cations were prepared as described in the literature or by straightforward modifications of the literature methods. The products were characterized by comparing their optical spectra (frequencies and extinction coefficients) with reported spectra.[1] In all cases agreement was excellent.

All procedures were carried out by standard Schlenk techniques under an argon atmosphere or in a He-atmosphere drybox equipped with a recirculating system. Solutions were protected from light, and solids were stored in a −35 °C freezer in the drybox. Optical spectra were measured in the range 210–650 nm using a Cary Model 14R spectrophotometer.

X-ray photoemission spectra were recorded with a HP 5950A spectrometer using monochromatized Al Kα radiation. The instrumental response function is very nearly gaussian with a fwhm value of 0.55 eV. Spectra were measured at pressures of $\sim 1 \times 10^{-9}$ Torr. An important factor in these experiments is the method by which the samples are prepared for measurement. In particular, appreciably different XPS spectra for the [II,III] bromide salt were observed depending on the method of sampling mounting. Four different procedures were used for the bromide and tosylate salts: (1) powder was pressed onto a Au-plated substrate, (2) powder was pressed onto a partially roughened Cu substrate, (3) methanol solutions were evaporated on Cu, (4) suspensions in hexane were evaporated on Au.

The effect of the sample mounting procedure on the [II,III] complex was monitored by dissolving the sample from the substrate in degassed 1 M $HClO_4$ under a He atmosphere and measuring the optical spectrum of the resulting solution. The solution was then exposed to air for ~0.5 h and the spectrum was remeasured. This procedure enables the reduction of [II,III] dimer to [II,II] species to be detected by the observation of a high-energy shift in the 18-kK band (this band occurs at 565 nm in the [II,III] complex and at 547 nm in the [II,II] dimer) followed by a corresponding shift to lower energy on exposure to air. Oxidation to the [III,III] species would be signaled by the appearance of an absorption near 352 nm. The effect of radiation exposure of the sample in the X-ray spectrometer was also checked by this procedure, but no changes other than those caused by the sample mounting techniques were detected; i.e., any radiation damage effects that were observed in the XPS spectrum were not observed in the optical measurements because only the surface region of the sample was affected.

Results

Ru 3d Spectrum: General Considerations. To point out the salient features of a Ru 3d X-ray photoemission spectrum we show in the bottom half of Figure 1 results from a $[RuCl(NH_3)_5]Cl_2$ sample prepared by gently pressing the powder onto a Au-plated substrate. The Ru $3d_{5/2}$ and $3d_{3/2}$ spin–oribt components of the Ru(III) species are separated by 4.2 ± 0.1 eV. Coster–Kronig lifetime broadening of the $3d_{3/2}$ state is responsible for the apparent discrepancy in the relative peak heights (the areas have the expected $(2J + 1)$ statistical weighting of 6:4). The C 1s photopeak appearing at 284.6 eV is primarily due to residual surface carbon from the substrate, which was rinsed with methanol and dried prior to sample mounting.

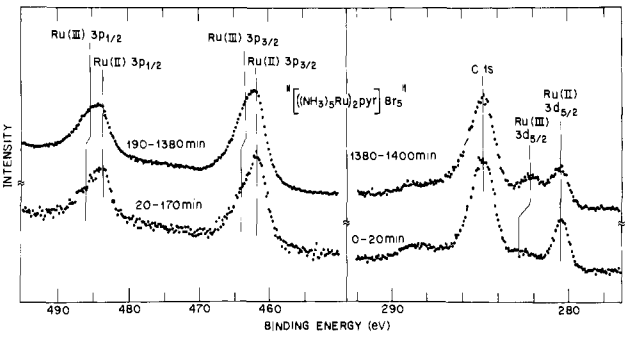

Figure 2. Ru 3d and 3p spectra from "nominal" mixed valence Creutz–Taube bromide salts taken as a function of X-radiation exposure. Samples mounted by pressing onto roughened Cu substrates. Note the difference between the 3d spectrum here and the spectrum in Figure 1 (top).

The upper half of Figure 1 shows the same energy region of an XPS spectrum from the mixed valence [II,III] bromide powder mounted in a similar fashion. Two pairs of spin–orbit Ru 3d core levels, each split by 4.2 ± 0.1 eV and corresponding to Ru(II) and Ru(III) species, are clearly seen. Their peak-to-peak binding energy difference (chemical shift) is 2.3 ± 0.1 eV. The C 1s photopeak, now primarily from the pyrazine ring and slightly shifted in energy from the C 1s peak in the $[RuCl(NH_3)_5]Cl_2$ sample, again makes accurate intensity assignments extremely difficult. In addition to obstruction from the C 1s level, it appears that the ratio of the Ru(II) and Ru(III) $3d_{5/2}$ absolute intensities is not 1:1. This is, however, misleading since it is the integrated peak intensities (areas) that are of importance. The reason for the apparent discrepancy is that the 3d hole state is broadened by exchange splitting in low-spin Ru(III) $4d^5$, while exchange splitting is absent in low-spin Ru(II) $4d^6$. In order to determine reliable relative intensity ratios between Ru(II) and Ru(III) species, therefore, it is clear that the 3d levels are inappropriate. The 3p levels, bound by an additional 180 eV, are more suitable because of the absence of C 1s interference and because of the reduced effect of exchange splitting. Intensity ratio analyses of the 3p levels are given at the end of this section.

Consideration of Artifactual Effects. We first look at the two most likely artifactual effects that could arise in XPS analysis of these mixed valence compounds, namely, sample change in the mounting procedure and X-radiation damage. The bottom spectra in Figure 2 show Ru 3d and 3p photoemission from the [II,III] bromide salt prepared by scraping the powder onto a partially roughened Cu substrate. This is a common procedure used in XPS studies of inorganic compounds. Note that only one Ru component is apparent in these spectra, suggesting a delocalized ground state for the [II,III] complex. Upon further exposure of this sample to X-radiation, an additional Ru component is observed (see top spectra in Figure 2). This result might suggest that the two-component spectra reported in ref 4 for the [II,III] complex resulted from radiation-induced decomposition.

There are, however, several difficulties with this interpretation. First, the earlier XPS 3d data of the tosylate salts[4] were taken in minutes, not the many hours required to observe a second component. Second, the peak-to-peak chemical shift between the Ru(II) and Ru(III) species is seen to decrease with increasing radiation exposure to 1.7 ± 0.1 eV, well outside the experimental uncertainty of 2.3 ± 0.1 eV found in Figure 1 for the [II,III] bromide and 2.7 ± 0.1 eV reported for the [II,III] tosylate in ref 4. Finally, there is the obvious fact that the single-component spectrum is virtually identical with the spectrum of the pure [II,II] compound. This is contrary to the expectation that the binding energy of a single-component [II1/2, II1/2] XPS spectrum, corresponding to a completely delocalized system, should be intermediate between the [II,II] and [III,III] photopeak energies. That this is not observed suggests that what was measured (and is shown in Figure 2) is actually a form of the [II,II] species.

To test this hypothesis we have measured the optical spectrum of a solution prepared from a [II,III] bromide sample that had been pressed onto a Cu substrate, but which had not been exposed to X-radiation. The results clearly indicate that the sample is reduced to a [II,II] species by

Table I. Effect of Sample Mounting Techniques on $[(NH_3)_5Ru(pyr)Ru(NH_3)_5]X_5$[a]

anion	technique	position of 18-kK band, nm: before exposure to air	position of 18-kK band, nm: after exposure to air	conclusion[b]
Tos^-	pressed onto Cu[c]	555	559[f]	partly reduced
Br^-	pressed onto Cu[c]	540	555[g] 561[h]	reduced
Br^-	evap of hexane suspension on Cu[d]	563		unchanged or slightly reduced
Tos^-	pressed onto Au[c]	565		unchanged
Tos^-	evap of MeOH soln on Cu[e]	564		unchanged

[a] X = Tos^- (p-$CH_3C_6H_4SO_3^-$), Br^-. [b] In no case was a band characteristic of the [III,III] dimer observed. [c] Pressed lightly with a stainless steel spatula and measured immediately after preparation. [d] Measured after about 8 h standing. [e] Measured about 1/2 h after preparation; the solution was not protected from light during evaporation. [f] 15-min exposure. [g] 10-min exposure. [h] 40 min exposure.

such a mounting procedure. The effects of radiation damage, which are readily apparent in the XPS spectra (Figure 2), were not detected in the optical absorption measurement because the surface region (<100 Å) from which the XPS spectra originate comprises a negligible fraction of the bulk material. The important conclusion from this result is that the procedure for mounting these mixed valence samples plays a critical role in their characterization. Previous interpretations of XPS spectra of mixed valence complexes where particular attention was not paid to the sample mountings procedure may need to be reexamined.[17]

With this established we investigated several methods for mounting these materials. Because of the absence of possible complicating effects from X-radiation in the XPS measurements, we relied primarily on optical spectroscopy for assessing their success. The results are summarized in Table I. It is clear that pressing the mixed valence complex onto a Cu plate reduces it. On the other hand, gently pressing the compound onto a Au surface, the procedure used in the earlier XPS study,[4] leaves it unchanged. Samples deposited on a Cu surface by evaporation from hexane suspension or methanol solutions are essentially unchanged if examined shortly after preparation. However, Cu surfaces are stained by the [II,III] complex on overnight standing so that samples deposited on Cu, even if initially satisfactory, may be expected to change with time. Gold surfaces are unaffected by the [II,III] complex and gentle pressing or evaporation from solution onto them leaves the samples unchanged. In all the work that follows we have therefore used Au-plated substrates.

To assess the importance of X-radiation damage of the samples, we made the following measurements. Samples of [II,III] bromide deposited from hexane suspension onto three separate Au-plated substrates were each analyzed in the Ru 3d region for approximately 0.5 min at an X-ray power of 0.2 kW (one-eighth the power used in the earlier XPS study with the same instrument[4]). The three results were added and compared with the sum of three spectra taken during the next 0.5 min. This procedure was repeated for 2 min, after which longer integration times were used. Representative results are shown in Figure 3. Because no spectral changes were observed within the first 2 min of exposure, all spectra taken during that time interval were added. Also, following the first 2 min of exposure the X-ray power was increased to 0.8 kW. Within the statistical uncertainty of the measurements no change in either peak position or intensity occurred during the radiation exposure times indicated in Figure 3. Longer exposure times of the order of 12 h (not shown) did result in a small decrease in binding energy (~0.4 eV) of the Ru(III) component as measured by the peak position. No significant relative intensity changes were observed within this time. Results of a similar study on the [II,III] tosylate salt are shown in Figure 4. It is seen that between 0 and 2 h the spectra remain unchanged, but for considerably longer exposures the [II,III] tosylate complex is reduced, as evidenced by the increase in the Ru(II)/Ru(III) intensity ratio. The Ru(II) and Ru(III) binding energies are unaffected. This behavior contrasts with that observed for the decomposed [II,III] Br compound (Figure 2) in which the Ru(II)/Ru(III) intensity ratio was observed to

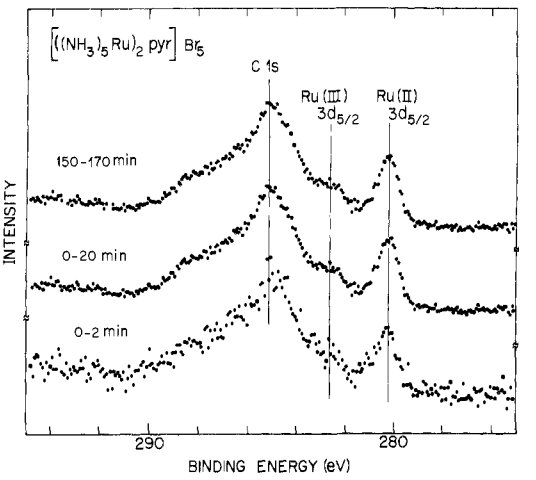

Figure 3. Ru 3d spectra from mixed valence Creutz–Taube bromide salt as a function of X-radiation exposure. Samples mounted on Au substrates from evaporated hexane suspensions. Note constancy of peak positions and intensities and contrast with Figure 2.

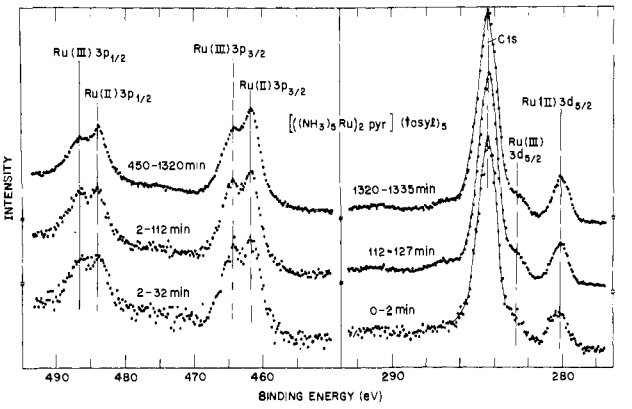

Figure 4. Ru 3d and 3p spectra from the mixed valence Creutz–Taube tosylate salt as a function of X-radiation exposure. Samples mounted on Au substrates. Note the constancy of peak positions and intensities within the first ~2 h and the slow degradation with longer exposures.

decrease with increasing radiation exposure, and with that observed for the true [II,III] Br compound upon longer exposures (not shown) in which the intensity ratio remained essentially constant. In both these latter cases the Ru(III) component binding energy also decreased with increasing exposure time. For our purposes, the important conclusion to be drawn from the above results is that radiation damage effects for both the bromide and tosylate salts become experimentally observable only for radiation exposures in our analyzer well in excess of 2 h with X-ray powers of ≤0.8 kW. We therefore regard the determination of relative integrated intensities of the Ru(II) and Ru(III) components measured within the conservative time frame of about 2 h to be free from radiation damage effects.

We have also considered the possible effects on the XPS spectra of sampling only the surface region, of temperature, of sample charging, and of exposure to moisture, air, and vacuum. All samples were stored at −35 °C and mounted in a He drybox. They were initially transferred into the XPS spectrometer under a dry inert atmosphere, but following the absence of any observable spectral differences upon rapid transfer (in a He-filled vial) to the spectrometer sample probe (in air), this latter procedure was ultimately adopted. Room-temperature samples left out in dry and moist air for periods of several hours also showed no measurable differences from those analyzed under the more controlled conditions. The lack of water of hydration in these systems makes the effect of vacuum unimportant. In order to assess the effects of sample charging, the thickness of the mounted samples was varied as well as the method of mounting (discussed above). The effects of significant inhomogeneous sample charging were observed for thick (~0.1 mm) materials, e.g., broad and ill-defined shapes, whereas thinner samples (<100 μ) showed no such behavior. Since the samples were in the form of finely divided powders with grain sizes clearly in excess of the effective core electron escape depths (<100 Å), no unambiguous distinction between surface and bulk properties in the nonradiation-damaged samples could be discerned. The only other surface–bulk differences that might be imagined are

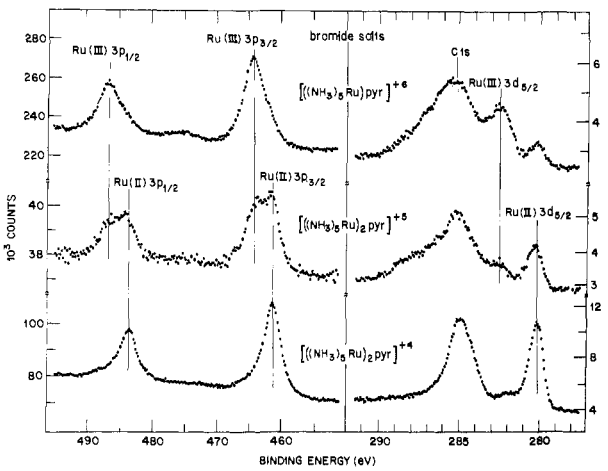

Figure 5. Ru 3d and 3p spectra from +4, +5, and +6 Creutz–Taube bromide salts. Samples mounted on Au substrates from evaporated hexane suspensions.

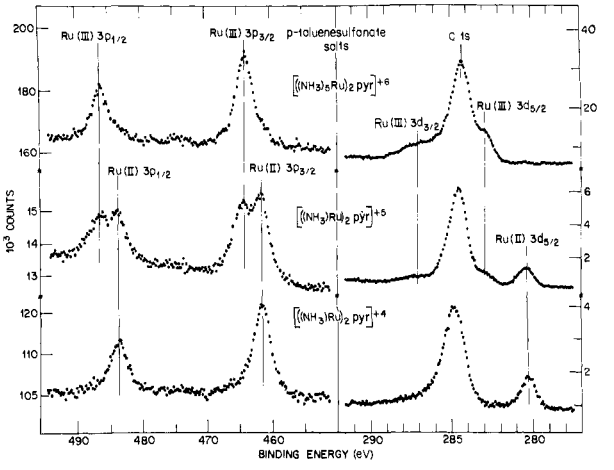

Figure 6. Ru 3d and 3p spectra from +4, +5, and +6 Creutz–Taube tosylate salts. Samples mounted on Au substrates.

surface vs. bulk Madelung corrections and the presence of surface contamination. The former effects are averaged out for these powdered complexes and the latter have been carefully monitored and found to be of little consequence.

Ru 3d and 3p Spectra. In Figure 5 we show the Ru 3d and 3p spectra of the [II,II], [II,III], and [III,III] bromide salts. The [II,III] Ru 3d spectrum here is the 0–20-min scan shown in Figure 3; the [II,III] Ru 3p spectrum was then recorded for an additional 130 min. No obvious effects of radiation damage on the [II,II] and [III,III] samples were observed, while the [III,III] salts were seen to be sensitive to pressure on Cu substrates resulting in formation of a reduced species. (Detailed studies of radiation damage effects and sample mounting were not undertaken for the [II,II] and [III,III] complexes.) The binding energies in the spectra shown in Figure 5 (and in all the spectra reported in this work) were not referenced to some standard core level (e.g., C 1s in graphite) because binding energies for irradiated insulators cannot be calibrated; i.e., the quasi-Fermi level of such a sample is not well defined.[18,19] For a given compound measured under a variety of conditions and at different times, binding energies were reproducible to within ±0.1 eV, suggesting minimal sample charging effects.

On the basis of our discussion of Figure 1, the assignment of the photopeaks in the [II,III] complex is straightforward. Two clearly resolved Ru $3d_{5/2}$ components separated by 2.3 ± 0.1 eV are apparent. The $3d_{3/2}$ components are obscured by the C 1s photopeak. As already stated, relative Ru 3d peak heights are not 1:1 because of C 1s obstruction and exchange splitting between the Ru (III) 3d and Ru (III) 4d electrons. The Ru 3p spectra, on the other hand, do indicate more nearly equal peak heights, but again because of exchange splitting the Ru(III) component is somewhat broader. The peak-to-peak chemical shift in the [II,III] bromide Ru 3p spectrum is 2.1 ± 0.1 eV, just within experimental error of the Ru 3d value (they need not be the same[20,21]). Least-squares analyses of the Ru 3p spectra for determining the relative integrated intensities and binding energies of the two components are discussed at the end of this section.

In Figure 6 we show the analogous Ru 3d and 3p spectra of [II,II], [II,III], and [III,III] *p*-toluenesulfonate salts. The Ru 3d and 3p spectra of the [III,III] compound were reproduced from the earlier XPS study;[4] the [II,II] and [II,III] complexes were remeasured. Unlike the earlier study, where the C 1s photopeaks (arising primarily from the tosylate anions) were arbitrarily aligned, the spectra are shown here with no adjustment of binding energy scales. This removes the small energy displacement (<0.2 eV) between the Ru(II) $3d_{5/2}$ components in the [II,II] and [II,III] salts found in the earlier work. Similar to the [II,III] Br salt, the Ru(III) $3d_{5/2}$ component in the [II,III] tosylate complex is readily apparent but difficult to characterize in any detail. The Ru 3p spectra, however, clearly demonstrate the existence of two well-resolved

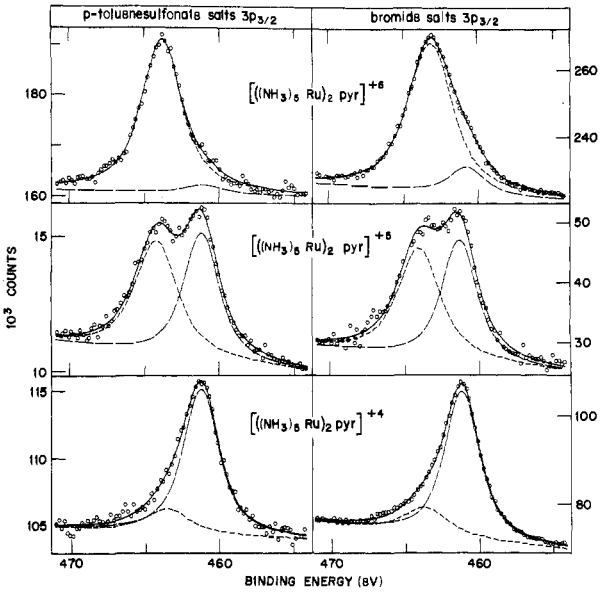

Figure 7. Least-squares analysis of the $3p_{3/2}$ component(s) in the +4, +5, and +6 Creutz–Taube bromide and tosylate salts. Weak components in the +4 and +6 spectra are due to impurities.

Ru components. The peak-to-peak chemical shifts here are the same for the 3d and 3p spectra, 2.7 ± 0.1 eV, a value somewhat larger than that observed in the [II,III] Br complex. In all respects (save the small difference in absolute binding energy scales) the spectra reported here for differently prepared and mounted samples are indistinguishable from those reported in the earlier XPS study.[4]

Least-Squares Analysis of Ru 3p Data. To make clear our approach in analyzing the Ru 3p data we note the following facts. The line shape in photoemission from nonmetallic materials (i.e., in which electron-hole pair production is absent) is described by a convolution of three contributions: the Lorentzian lifetime of the core hole state in question, the Gaussian broadening due to production of phonons, and the instrumental response function.[22] The latter quantity has been characterized previously as a slightly skewed Gaussian[23] and is not adjustable. For a single photopeak this leaves essentially two line-shape parameters, namely the widths of the simple Lorentzian and Gaussian distributions. In the mixed valence compounds the Ru(II) and Ru(III) components have different line shapes because of differences in exchange splitting, so there are now four adjustable widths to consider. In addition to the widths, we wish to describe the intensity and position of each line, increasing the number of adjustable parameters to eight. Add to this an adjustable background, and the problem of parameter correlation virtually precludes any possibility for a unique, physically reliable result for an unconstrained two-component fit. The approach taken, therefore, was first to fit the [II,II]

(18) The Fermi level for an nonirradiated insulator lies midway in the gap between the filled valence and unfilled conduction bands. Upon X-radiation, however, there is an effective Fermi level for electrons and for holes and its position is no longer well established.

(19) P. H. Citrin and T. D. Thomas, *J. Chem. Phys.*, **57**, 4446 (1972).
(20) P. H. Citrin, *Phys. Rev. B*, **8**, 5545 (1973).
(21) K. Siegbahn, *J. Electron Spectrosc. Relat. Phenom.*, **5**, 3 (1974).
(22) P. H. Citrin, G. K. Wertheim, and Y. Baer, *Phys. Rev. B*, **16**, 4256 (1977).
(23) G. K. Wertheim, *J. Electron Spectrosc. Relat. Phenom.*, **6**, 239 (1975).
(24) G. A. Sawatzky and A. Lenselink, *J. Chem. Phys.*, **72**, 3748 (1980).

Table II. Summary of Least-Squares Analysis of Ru $3p_{3/2}$ Component in Binuclear Ruthenium Compounds[a]

compound		$\Gamma_{3p_{3/2}}$,[b] eV	Γ_{ph},[c] eV	BE,[d] eV	ΔBE,[e] eV	I[f]
[III,III] Tos	III	1.30	1.19	464.26	2.87	0.956
	II[g]	(1.00)[h]	(1.41)[h]	461.39		0.044
[III,III] Br	III	1.31	1.75	463.56	2.52	0.873
	II[g]	(1.00)[h]	(1.41)[h]	461.04		0.127
[II,II] Tos	III[g]	(1.30)[h]	(1.47)[h]	463.77	2.26	0.166
	II	1.02	1.43	461.51		0.834
[II,II] Br	III[g]	(1.30)[h]	(1.47)[h]	463.89	2.48	0.179
	II	0.97	1.39	461.41		0.821
[II,III] Tos	III	(1.30)[h]	(1.47)[h]	464.62	3.07	0.514
	II	(1.00)[h]	(1.41)[h]	461.55		0.486
[II,III] Br	III	(1.30)[h]	(1.47)[h]	464.31	2.77	0.516
	II	(1.00)[h]	(1.41)[h]	461.54		0.484

[a] Relative values within a given compound are more meaningful than absolute values. [b] Fwhm Lorentzian lifetime. [c] Fwhm Gaussian phonon broadening. [d] Binding energy (see footnote *a*). [e] Chemical shift (Ru(II)–Ru(III)). [f] Fractional integrated intensity. [g] Impurity component. [h] Constrained.

and [III,III] data and then use the appropriately determined lifetime and phonon line widths as fixed input parameters in the fits of the mixed valence [II,III] data. The advantage of this procedure in halving the number of adjustable parameters and thus allowing a feasible fit more than outweighs the disadvantage of modelling the Ru(II) and Ru(III) line shapes in the [II,III] compounds. This is so because, while some differences in line shapes are expected between the single oxidation state and the mixed valence systems of a given anion, the negligible changes in binding energies between the two cases suggest that such line-shape differences are small. Two other minor approximations in the fitting approach are that the background is assumed to be linear over the rather narrow region of energy fit (~15 eV) and that the effect of exchange splitting in the Ru(III) hole state (it is considerably smaller than the line width) is approximated by additional broadening.

The results of the least-squares analysis of the Ru $3p_{3/2}$ component are summarized in Figure 7 and Table II. Because of the presence of small amounts of reduced species in the [III,III] samples and of oxidized species in the [II,II] samples (due either to original impurity or introduced as a result of sample mounting), it was necessary to fit the spectra iteratively, i.e., to alternately constrain the line shapes of the minor impurity components until self-consistency was obtained. The excellent agreement between the Lorentzian widths in the [II,II] and [III,III] bromide and tosylate salts (see Table II) is gratifying. The same statement applies to the Gaussian widths in the two [II,II] compounds. The difference in Gaussian widths in the two [III,III] compounds is presumably due in large measure to our having approximated the exchange splitting by a simple broadening. Exchange splitting may indeed be different between the bromide and tosylate [III,III] compounds, as already suggested by the difference in Ru(II)–Ru(III) chemical shifts and the Ru(III) $3d_{5/2}$ widths in the [II,III] systems (see Figures 4 and 5). Furthermore, the difference in Lorentzian widths between the [II,II] and [III,III] salts, even if self-consistent, does not reflect real differences in hole-state lifetimes but rather reflects again our approximation of exchange splitting as a broadening. In the interest of simplicity—and because such effects are of only secondary importance in determining the relative intensities—the mean values of the Gaussian and Lorentzian widths determined from the four single oxidiation state complexes were used in fitting the [II,III] bromide and tosylate salts. The relative integrated intensities of the photopeaks are given in the last column of Table II. It is clear that in both mixed valence compounds the areas of the Ru(II) and Ru(III) components are virtually identical (their similarity between compounds is fortuitous). Varying the line-shape parameters within the broadest limits that are still compatible with the single oxidation state data results in changes of the Ru(II):Ru(III) area ratios of less than ±8%. A conservative estimate of the relative Ru(II):Ru(III) integrated intensities is 1.0:1.0 ± 0.1. The chemical shift is similarly insensitive to such variations in the line-shape parameters. This applies even to the chemical shifts in the single oxidation state compounds, which are certainly less reliable because of the relatively poorly determined positions of the impurity components. It should also be noted that the chemical shifts of the [II,III] compounds in Table II are somewhat larger than the peak-to-peak values quoted in the previous discussions of Figures 1, 4, and 5. On the one hand, this difference is due to the misleading effects of determining positions of closely separated convoluted components, thereby favoring the least-squares results. On the other hand, the constrained position of the components as a result of their approximated line shapes would tend to favor the somewhat smaller peak-to-peak binding energy values. We therefore quote conservative estimates of the Ru(II)–Ru(III) chemical shifts of 2.8 ± 0.3 eV for the [II,III] tosylate and 2.5 ± 0.3 eV for the [II,III] bromide.

Discussion

Intersite electron exchange of the trapped valence in a class II complex should be slow on the very short XPS measurement time scale so that an asymmetric ground state is expected to yield two peaks of equal integrated intensity, one near the binding energy of the low oxidation state metal center and the other near the binding energy of the high oxidation state. This is precisely what we have observed for the Creutz–Taube mixed valence complex. However, Hush[7] has shown that a similar spectrum could arise for a class III complex because the valence orbital, which is delocalized in the ground state, becomes localized in the photoionized state. To determine if our XPS measurements can distinguish between the two cases, it is necessary to make a detailed comparison of the results with Hush's model. We do this by comparing the results with the model as originally proposed[7] and with a modified version, presented below, which allows for different electron interaction integrals in the ground and photoionized states. We now derive this modified model.

Following Wong and Schatz,[14] consider a mixed valence dimer and label the two equivalent halves (subunits) of the molecule A and B (A = B). Let the formal oxidation states which can be associated with the metal atoms in the molecule be L and M (L < M) and, depending on the associated oxidation state, write the wave functions for the subunits as ψ_L^A or ψ_M^A and ψ_L^B or ψ_M^B. In the absence of interaction between the two halves of the molecule, the composite system will have two degenerate states which can be written

$$\psi_a = \psi_L^A\psi_M^B \qquad \psi_b = \psi_M^A\psi_L^B \tag{1}$$

The degeneracy of these states is lifted both by coupling to the totally symmetric vibration associated with each subunit and by electronic interaction between the subunits. If we allow for both vibration and electronic coupling, the energies of the states are given by

$$E_\pm = \tfrac{1}{2}kq^2 \mp (J^2 + g^2q^2)^{1/2} \tag{2}$$

where g is the vibronic coupling constant, k is the force constant for the totally symmetric vibration, q is the appropriate normal coordinate,[14] and J is the electronic coupling integral given by

$$J = \langle\psi_a|H_{el}|\psi_b\rangle \tag{3}$$

The corresponding electronic wave functions are

$$\psi_\pm = c_a^\pm\psi_a + c_b^\pm\psi_b \tag{4}$$

with

$$c_a^\pm = J\{[gq \pm (J^2 + g^2q^2)^{1/2}]^2 + J^2\}^{-1/2} \tag{5}$$

$$c_b^\pm = [gq \pm (J^2 + g^2q^2)^{1/2}]\{[gq \pm (J^2 + g^2q^2)^{1/2}]^2 + J^2\}^{-1/2} \tag{6}$$

The condition for a delocalized system is that the ground-state energy surface have only a single minimum. From eq 2 it is evident that this occurs when $J > g^2/k$ and that the minimum is at $q = 0$. The ground-state wave function for a delocalized system at the energy minimum is therefore

$$\psi_+(N) = \frac{1}{\sqrt{2}}(\psi_a(N) + \psi_b(N)) \tag{7}$$

where we have now explicitly noted that the system contains N electrons.

Next consider the mixed valence dimer after a metal atom core electron has been removed (photoionized state), and assume that the core hole is localized[24] on the metal atom in subunit A. The two subunits are no longer equivalent (A ≠ B) so that even in the absence of interaction, the states $\psi_a^{ion}(N-c)$ and $\psi_b^{ion}(N-c)$ are not degenerate (the notation N–c is used to indicate explicitly that a core electron has been removed). $\psi_a^{ion}(N-c)$ describes a state in which the core hole and the (M–L) valence electrons are localized on subunit A, while in state $\psi_b^{ion}(N-c)$ the (M–L) valence electrons are on subunit B and the core hole remains in A. If we allow for both vibration and electronic coupling, $\psi_a^{ion}(N-c)$ and $\psi_b^{ion}(N-c)$ mix and the two lowest energy states of the photoionized system are now described by

$$\psi_\pm^{ion}(N-c) = c'_a{}^{\pm}\psi_a^{ion}(N-c) + c'_b{}^{\pm}\psi_b^{ion}(N-c) \quad (8)$$

with coefficients

$$c'_a{}^{\pm} = J'\left\{\left[g'q + \frac{\Delta'}{2} \pm \left(J'^2 + \left(g'q + \frac{\Delta'}{2}\right)^2\right)^{1/2}\right]^2 + J'^2\right\}^{-1/2} \quad (8a)$$

$$c'_b{}^{\pm} = \left[g'q + \frac{\Delta'}{2} \pm \left(J'^2 + \left(g'q + \frac{\Delta'}{2}\right)^2\right)^{1/2}\right]\left\{\left[g'q + \frac{\Delta'}{2} \pm \left(J'^2 + \left(g'q + \frac{\Delta'}{2}\right)^2\right)^{1/2}\right]^2 + J'^2\right\}^{-1/2} \quad (8b)$$

and eigenvalues

$$E_\pm^{ion} = \frac{1}{2}k'q^2 \mp \left[J'^2 + \left(g'q + \frac{\Delta'}{2}\right)^2\right]^{1/2} \quad (9)$$

The primes in eq 8 and 9 are used to emphasize that the quantities refer to the photoionized state; in particular

$$J' = \langle\psi_a^{ion}(N-c)|H'_{el}|\psi_b^{ion}(N-c)\rangle \quad (10)$$

and Δ' is the difference in energy between the states $\psi_b^{ion}(N-c)$ and $\psi_a^{ion}(N-c)$ (no interaction).

From the ground state minimum ($q = 0$), there is an allowed photoionization transition to each of the states of eq 8; these occur at binding energies

$$E_1 = E_+^{ion} - E_+ = -\left[J'^2 + \frac{\Delta'^2}{4}\right]^{1/2} + J \quad (11)$$

and

$$E_2 = E_-^{ion} - E_+ = \left[J'^2 \frac{\Delta'^2}{4}\right]^{1/2} + J \quad (12)$$

The zero of energy for eq 11 and 12 is the average binding energy for the transitions from the ground state ($q = 0$) to noninteracting states $\psi_a^{ion}(N-c)$ and $\psi_b^{ion}(N-c)$. In the original Hush model,[7] the equations corresponding to eq 11 and 12 have the same J, the ground-state coupling integral, both inside and outside the brackets.

A formula for the relative intensities of the photoionization peaks with binding energies E_1 and E_2 is readily derived with the aid of the sudden approximation. In this approximation the probability that a core photoionization event will result in a particular state $\psi_\pm^{ion}(N-c)$ is[25]

$$P_\pm = |\langle\psi_\pm^{ion}(N-c)|\psi^{froz}(N-c)\rangle|^2 \quad (13)$$

where $\psi^{froz}(N-c)$ is the frozen state wave function for the ion, i.e., the molecule ground state wave function with a core hole:

$$\psi^{froz}(N-c) = \frac{1}{\sqrt{2}}(\psi_a(N-c) + \psi_b(N-c)) \quad (14)$$

$\psi_a(N-c)$ and $\psi_b(N-c)$ correspond to unrelaxed ground-state functions after removal of the core electron. The ratio of the intensity of the low binding energy peak to the high binding energy peak is therefore

$$\frac{P_+}{P_-} = \frac{1 + 2c'_a{}^{+}c'_b{}^{+}}{1 + 2c'_a{}^{-}c'_b{}^{-}} \quad (15)$$

In deriving eq 15 we have assumed that

$$\langle\psi_a^{ion}(N-c)|\psi_a(N-c)\rangle = \langle\psi_b^{ion}(N-c)|\psi_b(N-c)\rangle \quad (16a)$$

and

$$\langle\psi_a^{ion}(N-c)|\psi_b(N-c)\rangle = \langle\psi_b^{ion}(N-c)|\psi_a(N-c)\rangle \approx 0 \quad (16b)$$

If we define

$$\alpha = 2J'/\Delta' \quad (17)$$

and make use of the fact that $c'_2{}^{+}c'_b{}^{+} = -c'_a{}^{-}c'_b{}^{-}$, eq 15 may be written in the form

$$\frac{P_+}{P_-} = \left[\frac{1 + (\alpha^2 + 1)^{1/2} + \alpha}{1 + (\alpha^2 + 1)^{1/2} - \alpha}\right]^2 \quad (18)$$

Equation 18 is identical with the corresponding equation in the original Hush model,[7] with the very important exception that α is now defined in terms of the electronic coupling in the photoionized state rather than the ground state.

We can now compare our XPS results with Hush's model and with the modified Hush model just described. The most significant comparison is between the relative intensities that are observed and those given by eq 18. Figure 8 is a plot of P_-/P_+ against J', as given by eq 18; Δ' was taken to be 2.8 eV, the binding energy difference between Ru(III) and Ru(II) as measured from the [III,III] and [II,II) tosylate salts (Table II). The shaded area on the plot encompasses the J' values and intensity ratios consistent with our measurements. It is clear from Figure 8 that the ground-state value for the exchange coupling constant, 0.39 eV,[7,14] corresponds to an intensity ratio far outside the range consistent with experiment. If we restrict ourselves to the original Hush model we would be forced to conclude that only a localized ground state is consistent with the observed range for the intensity ratio. However, when we recognize that P_+/P_- is actually a function of J', the coupling in the photoionized state, and not of the ground state J, and that J' is expected to be much less than J,[26] we can

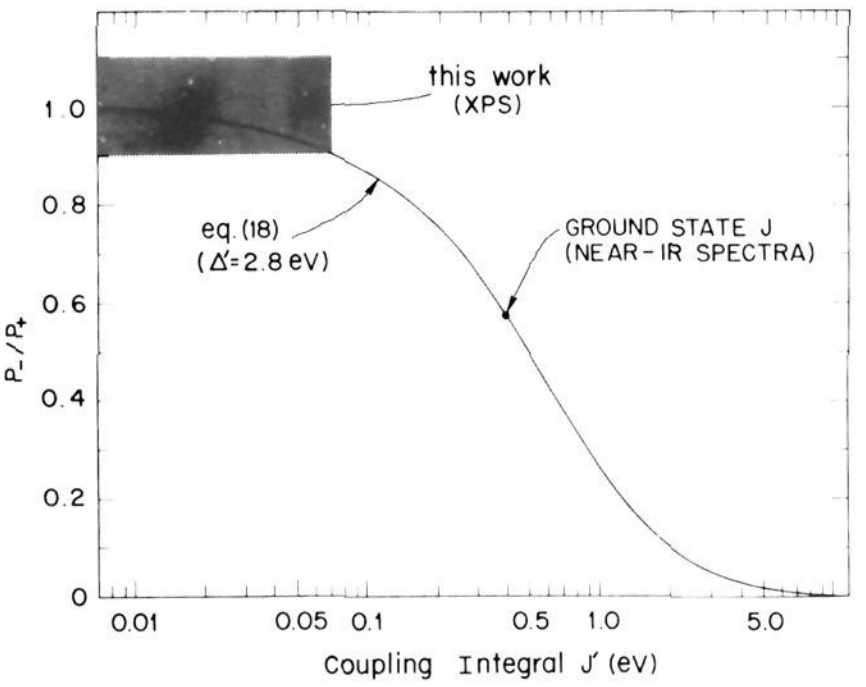

Figure 8. Theoretical curve (eq 18) giving the intensity ratio (high-binding energy peak/low-binding energy peak) for the Ru photopeaks in the [II,III] dimer spectrum as a function of coupling in the photoionized state. The shaded area delineates the range of intensity ratios and coupling integrals consistent with experiment. The curve is dashed in the high J' region to indicate that the model is inappropriate when J' is too large.

(25) R. Manne and T. Åberg, *Chem. Phys. Lett.*, **7**, 282 (1970).

no longer claim that the observed intensity ratio is inconsistent with a delocalized ground state. If indeed the ground state is delocalized we can conclude from Figure 8 that J' is in the range 0–0.07 eV.

It is interesting to note that eq 11 and 12 provide, in principle, a method for determining both the ground- and excited-state coupling integrals from XPS binding energies. Thus, we may write

$$J = \tfrac{1}{2}(E_1 + E_2) \tag{19}$$

and

$$J' = \tfrac{1}{2}[(E_2 - E_1)^2 - \Delta'^2]^{1/2} \tag{20}$$

Unfortunately, to obtain reliable values for the coupling integrals from eq 19 and 20 would require absolute binding energies considerably more accurate than can be measured from irradiated insulators.[18,19] A realistic estimate of such binding energy accuracies is at least ±0.1–0.2 eV for a given measurement. Since this uncertainty enters eq 19 and 20 via both the measurements on the mixed valence compound and also the reference compounds used to establish the energy zero for E_1 and E_2 and to obtain Δ', it is clear that these equations cannot, in practice, be used to estimate J and J' for a weakly coupled insulator.

We may summarize our conclusions as follows. A mixed valence dimer with a delocalized ground state (class III complex) but relatively weak metal–metal interaction will have an X-ray photoemission spectrum indistinguishable from a class II complex. The nature of the ground state of the Creutz–Taube mixed valence dimer therefore cannot be decided from XPS measurements. Hush's model in its original form[7] led to a similar conclusion, but suggested that careful relative XPS peak intensity measurements would permit the two cases to be distinguished. We have shown that the Hush model must be modified to allow for the expected large difference in electron coupling in the ground and photoionized states. When this is done it is found that a class III dimer with relatively weak metal–metal interaction should always give two photoemission peaks with 1:1 intensity; relative intensity measurements therefore cannot distinguish this case from a class II dimer. Binding energies, although they are related to the coupling in both the ground and photoionized states, also cannot be used to evaluate the coupling because of inherent limitations on the accuracy with which they can be measured in an insulator.

Finally, we wish to note that the basic idea of the Hush model, namely, the localization of a delocalized ground state by core hole polarization in the photoionized state, is anticipated in the work of Friedel[27] and of Combescott and Nozieres[28] on metals. These authors show that core hole polarization in the photoionized state can cause an electron from the conduction band to become localized in a level below the band. This theory has been used to account, at least qualitatively, for unexpected splittings in the XPS of metallic sodium tungsten bronzes.[29]

(26) Orbital contraction in the photoionized state should greatly reduce the interaction between the two Ru atoms. In this connection we note that magnetic susceptibility measurements on the [III,III] dimer show that coupling between the two Ru(III) centers is negligible;[11] we would expect that the coupling between the two metal atoms in the photoionized state is even smaller than the Ru(III)-Ru(III) coupling.

(27) J. Friedel, *Comments Solid State Phys.*, **2**, 21 (1969).
(28) M. Combescott and P. Nozieres, *J. Phys. (Paris)*, **32**, 913 (1971).
(29) J. N. Chazalviel, M. Campagna, G. K. Wertheim, and H. R. Shanks, *Phys. Rev. B*, **16**, 697 (1977).

Conformational Analysis of Polysubstituted Ethanes

Giorgio Favini, Massimo Simonetta,* and Roberto Todeschini

Contribution from the Institute of Physical Chemistry and Centro C.N.R., University of Milan, via Golgi 19, 20133 Milano, Italy. *Received September 30, 1980*

Abstract: Empirical force field (EFF) calculations were performed for a number of polyarylsubstituted ethanes and the ground state geometry and strain energy were obtained. Optimal geometrical parameters are compared with experimental data from X-ray crystal-structure determination. The agreement is extremely good for bond lengths and bond angles. Significant discrepancies may occur for dihedral angles, probably due to the effect of packing forces in the crystalline phase.

The empirical force field method has become a quite reliable and widely accepted tool for the determination of structure and energy of organic molecules, specially hydrocarbons. Its merit and drawbacks and the limit of applicability have been reviewed and discussed many times.[1] Recently particular attention has been paid to arylethanes, and molecular mechanics has been extensively used in the static and dynamic analysis of the stereochemistry of a number of members of the family.[2] One of the most interesting results from the theory is the ground state geometry of the molecules under study and perhaps the most reliable test for the adopted potential and parametrization is the comparison with the geometry obtained by experiment of some kind. The size of the molecules considered here is such that the source of experimental data is almost completely restricted to X-ray diffraction.

Particular attention must be taken here since the calculations refer to an isolated molecule, while X-ray data describe the molecules packed in the crystal. The comparison is particularly meaningful when packing is not too tight, that is not too many intermolecular distances fall below the sum of the van der Waals radii, and when the molecule is "rigid". The definition of rigidity should be related to a complete normal mode analysis for the isolated molecules and to a lattice dynamics study of the crystal.[3] In rigid molecules vibrational frequencies for internal modes should

(1) (a) J. E. Williams, P. J. Stang, and P. v. R. Schleyer, *Ann. Rev. Phys. Chem.*, **19**, 531 (1968); (b) E. M. Engler, J. D. Andose, and P. v. R. Schleyer, *J. Am. Chem. Soc.*, **95**, 8005 (1973); (c) N. L. Allinger, *Adv. Phys. Org. Chem.*, **13**, 1 (1976).
(2) (a) P. Finocchiaro, D. Gurt, W. D. Hounshell, J. P. Hummel, P. Maravigna, and K. Mislow, *J. Am. Chem. Soc.*, **98**, 4945 (1976); (b) P. Finocchiaro, W. D. Hounshell, and K. Mislow, *ibid.*, **98**, 4952 (1976); (c) W. D. Hounshell, D. A. Dougherty, J. P. Hummel, and K. Mislow, *ibid.*, **99**, 1916 (1977); (d) D. A. Dougherty, F. M. Llort, and K. Mislow, *Tetrahedron*, **34**, 1301 (1978); (e) D. A. Dougherty and K. Mislow, *J. Am. Chem. Soc.*, **101**, 1402 (1979).
(3) (a) G. Filippini, C. M. Gramaccioli, M. Simonetta, and G. B. Suffritti, *J. Chem. Phys.*, **59**, 5088 (1973); (b) G. Filippini, C. M. Gramaccioli, M. Simonetta, and G. B. Suffritti, *Chem. Phys.*, **8**, 136 (1975).

0002-7863/81/1503-3679$01.25/0